24th COBEM - 2017

24th ABCM International Congress of Mechanical Engineering
December 3-8, 2017, Curitiba, PR, Brazil

COBEM-2017-1242
CFD ANALYSIS OF GREASE FLOW BEHAVIOR FROM LABYRINTH SEALS

Luciano Frose
Universidade Tecnologica Federal do Parana
frose@alunos.utfpr.edu.br

Tiago Cousseau
Universidade Tecnologica Federal do Parana
tcousseau@utfpr.edu.br

Abstract. *In this study the grease flow behavior inside labyrinth mechanical seals is studied. The Herschel-Bulkley rheological model was used together with the Papanastasiou model for the numerical simulation. The numerical methodology was validated with the analytical solution of pressure-driven flow between to parallel plates for three types of grease with distinct rheological values. Different geometries of radial and axial labyrinth seals were analyzed. It was shown that axial mounted labyrinths remain more efficient due to more proximity with the rotation axis and therefore a smaller increase on the area in the radial direction, that would elevate the friction factor.*

Keywords: *Labyrinth Seals, CFD analysis, grease rheology*

1. INTRODUCTION

One of the many difficulties in the bearing industry is to provide sealing solutions for applications on highly intrusive environments, such as in the metal processing, mining, mineral, pulp and paper industries. The ingress of contaminants in rolling bearings can significantly reduce the service lifetime (Miskovic *et al.* (2016)).

Grease is widely used as lubricant and as well as sealing medium against contamination and leakage. Its use on labyrinth seals increases the tightness of the conveyour roller. This characteristics puts some difficulties to analyze the grease flow behavior, which is related to its sealing action, in complex geometries. However, by using Computational Fluid Dynamic (CFD) technique and a proper equation to describe grease flow, one can easily analyze the relationship among labyrinth geometry, grease flow and contamination entrance.

Yield stress has been widely studied in the past few decades, until today most of the analysis have adopted the flow criteria (Fernandes (2015)). Some authors discuss its existence stating that, under yield stress, the material is flowing at low shear rate, but it is not static (Barnes and Walters (1985)). Besides, even with all studies on this topic, (Nguyen, Q. D. D., 1992) recognizes the importance of the yield stress in the industry.

(Dobrowolski *et al.*, 2016) performed an experimental study measuring the grease inside a labyrinth gap using μPIV. This technic allows measurements of the grease bulk flow only up to 0,8 mm from the surface and therefore can be used to validade computational models.

This work concentrates on a numerical analysis of the grease velocity and pressure distribution inside a labyrinth seal geometry. Several labyrinth geometries with different greases are evaluated. Both cases, i.e. rotating and stationary (during churning process) are approached. The results were validated with tests performed in the μPIV-DRS test rig (Dobrowolski *et al.* (2016)).

2. COMPUTATIONAL PROCEDURE

All the flow behavior inside the labyrinth geometry can be described by solving the equations of motion, that in the vector form is written as following:

$$\rho\frac{D\mathbf{u}}{Dt} = \rho\frac{\partial\mathbf{u}}{\partial t} + \rho(\mathbf{u}\cdot\nabla)\mathbf{u} = -\nabla p + \rho\mathbf{F} + \nabla\cdot\tau \tag{1}$$

Where ρ is the grease density, D/Dt it the material derivative, $\mathbf{u}$ the velocity vector, p the pressure, $\mathbf{F}$ the volume force and τ the shear stress tensor.

After a relation between shear rate ($\dot{\gamma}$) and shear stress (τ) is applied, Eq. 1 is then called as the Navier-Stokes

equations. At low to moderate shear rates the grease the grease can be numerically adjusted using a modified Herschel-Buckley model Gonçalves *et al.* (2015).

$$\tau = \tau_y + K\dot{\gamma}^n \tag{2}$$

Where τ is the shear stress tensor, τ_y is the yield stress, $\dot{\gamma}$ the shear rate, K is the consistency index and n the the shear thinning/thickening exponent which for greases would usually be less than one, meaning that the apparent viscosity decreases which increasing shear rate.

Since the viscosity can be isolated from Eq. 2, it is possible to change the Newtonian viscosity on the Navier-Stokes equations with the following representing the Herschel-Buckley model.

$$\eta = \frac{\tau_y}{\dot{\gamma}} + K\dot{\gamma}^{n-1} \tag{3}$$

Where η is the apparent viscosity.

In order to have a continuous transition between elasticity and viscous region the Papanastasiou model is used. Plastic-viscous transition is a discontinuous function and therefore leads to numerical instability and computational errors.

$$\eta = \frac{\tau_y}{\dot{\gamma}}(1 - \exp(-m\dot{\gamma})) + K \tag{4}$$

where m is a smoothing parameter. By applying the Papanastasiou numerical model to describe the grease flow, the viscosity and shear response of the grease as function of the shear rate approaches the curves shown in Fig 1.

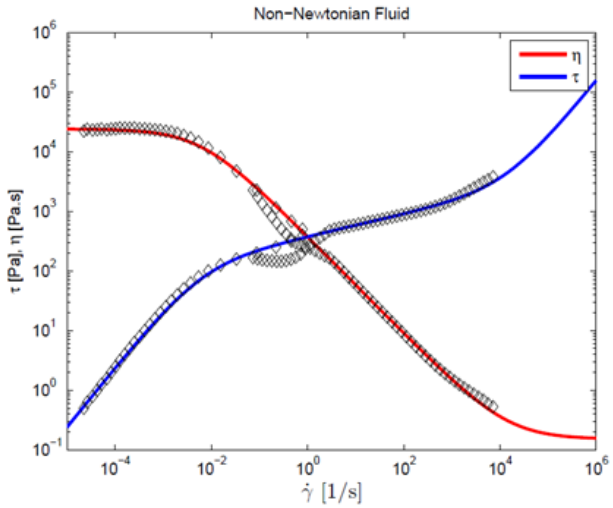

Figure 1: Shear stress measured from low to high shear rates (Cousseau (2013)).

Therefore, Eq. 1 was solved together with the Papanastasiou model (Eq. 4) using the FLUENT solver with a User Defined Function (UDF) for the apparent viscosity.

In order to validate the proposed UDF, a simplified two parallel plates geometry with a given inlet pressure is solved numerically and analytically. To do so the grease properties presented by Westerberg are used (Lars Westerberg, Erik Höglund, 2016). These properties are presented in Tab 1.

It is important pointing out that Lars Westerberg, Erik Höglund (2016) also simulated the parallel plates geometry with the lubricating greases described in Tab 1. Therefore their results will also be used to validate the proposed model.

Table 1: Data from cone-plate rheometer for three lithium soap greases (Westerberg *et al.*, 2017).

	τ_y[Pa]	K[Pa·sn]	n[-]
NLGI 00	0	1.85	1
NLGI 1	189	4.1	0.797
NLGI 2	650	20.6	0.605

All the simulations where carried out with FLUENT v16.0 using an UDF (User Defined Function) for the Papanastasiou model for the three lubricating greases presented in Table 1. A mesh density of 740 volumes/mm2, a smoothing parameter equals to 100000 and Three different inlet pressure values of 30, 140 and 240 kPa were used.

In order to validate the UDF, a numerical simulation was carried out for comparison with the analytical pressure-driven flow between two parallel plates. Fig. 2 demonstrate high quality capturing the unyielded regions. The result was a value of the mesh density of 740 volumes/mm^2 and a smoothing parameter equals to *100000*.

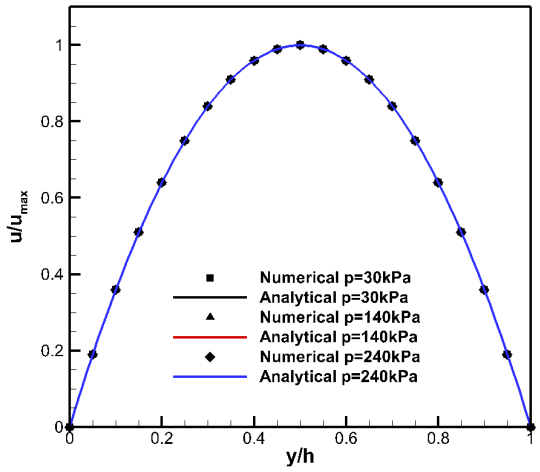

(a) NLGI 00

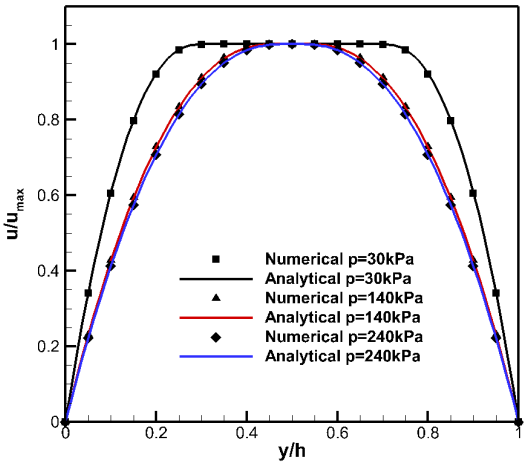

(b) NLGI 1

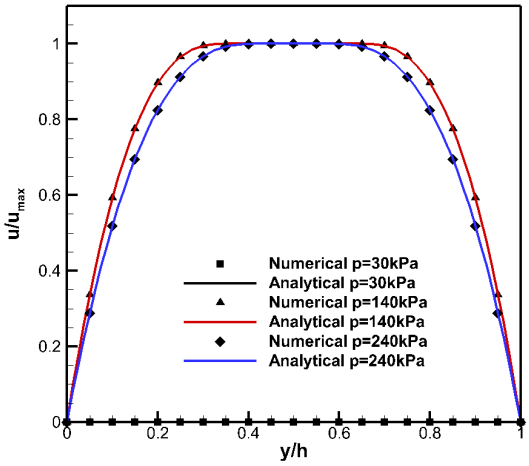

(c) NLGI 2

Figure 2: Comparison between analytical and numerical solutions for grease pressure drive flow between parallel plates.

3. Geometries and Boundary Conditions

Following the sugested dimensions from Kümmel and Werner (2010) for labyrinth seals the following axisymmetric geometries were studied. Maintaining the clearance constant on the radial and axial direction one can understand the influence of the assembly itself more clearly.

In order to understand the influence if one should choose a axial or radial labyrinth the total perimeter of the seal is constant, only adding more curves. Maintaining the perimeter is possible to compare the physical differences between each flow behavior and its advantages.

Figures 3a and 3b demonstrate the studied geometries. The problem was modeled as a 2D swirl axisymmtric laminar flow. A fixed difference pressure of $10kPa$ was maintained, together with a rotation of $400\ rpm$, usual for the size of the labyrinth studied. Since the NLGI 2 is the most common grease used it was the only one considered on this first step of the study (Cousseau, 2013).

Figure 4 exemplifies a mesh used for the radial double labyrinth.

Figure 5 demonstrates that although the mass-flow-rate for radial labyrinths are higher, there is a decrease when more curves are added, on the other hand for the axial geometries it remains constant.

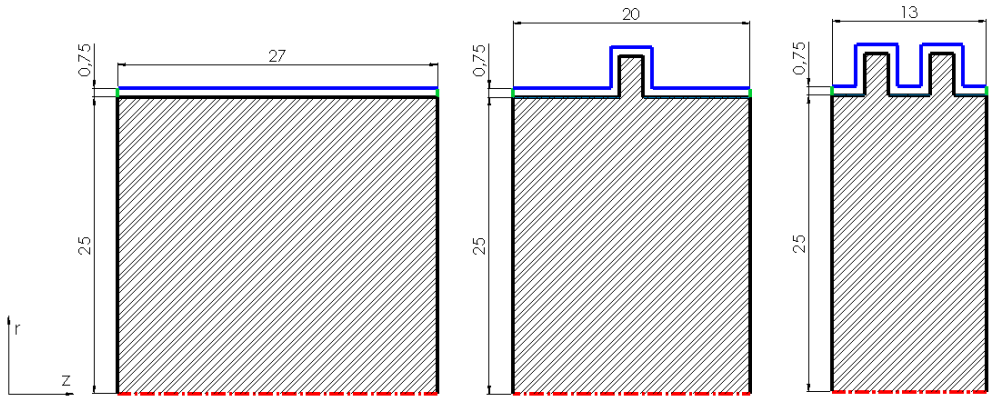

(a) Axial labyrinth geometries with boundary conditions. From left to right: straight, single and double axial labyrinth.

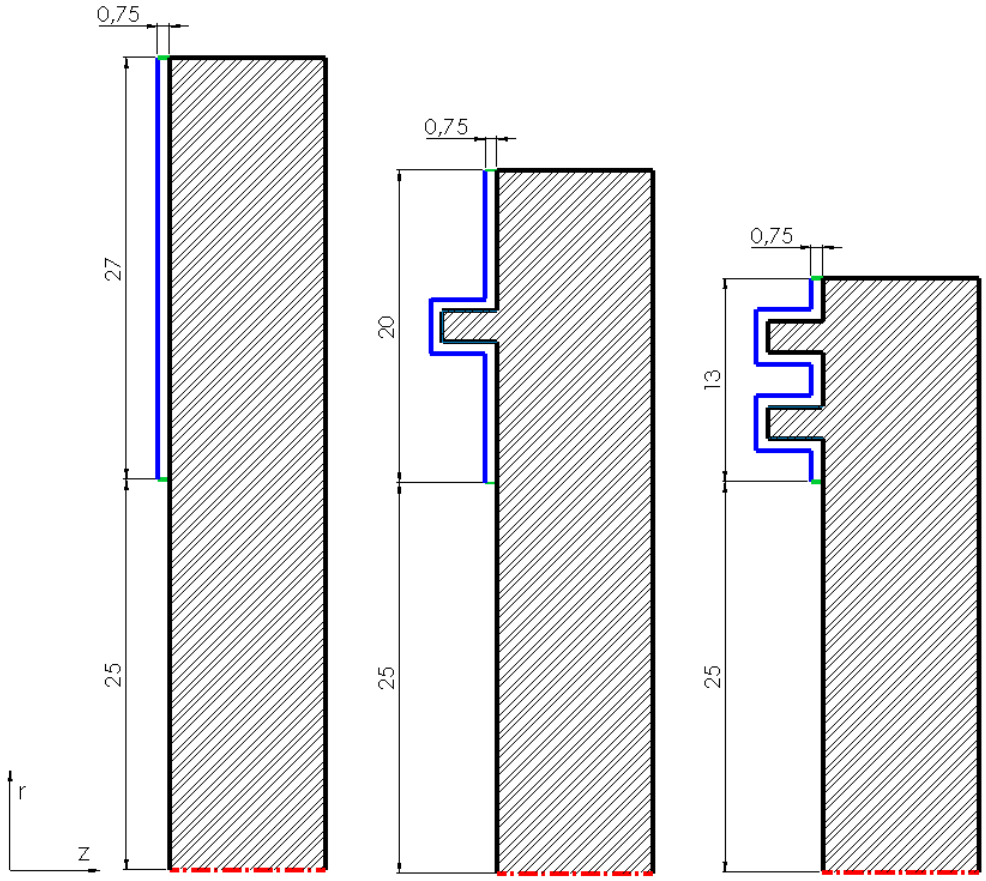

(b) Radial labyrinth geometries with boundary conditions. From left to right: straight, single and double radial labyrinth.

Figure 3: Axial and radial geometries with boundary conditions. *Red line*: axis of rotation, *Blue line*: housing part of the labyrinth, stationary, *Black lines*: shaft and labyrinth part that rotates mounted rotating wit the same angular speed, *Green line*: inlet and outlet of the labyrinth (axial: inlet on the left, radial: inlet on the surface near the axis)

A similar behavior is noticed on Figure 6 when comparing the viscous momentum for maintaining the constant rotation. Both of the phenomena can be explained with a better understanding of the behaviour from the velocity and the dynamic pressure.

Figure 6 indicates the difference of the dynamic pressure between a straight and radial labyrinth. One can notice that for the first case the pressure drops almost constantly when compared with the second case. It will only be a linear pressure drop when no rotation is present.

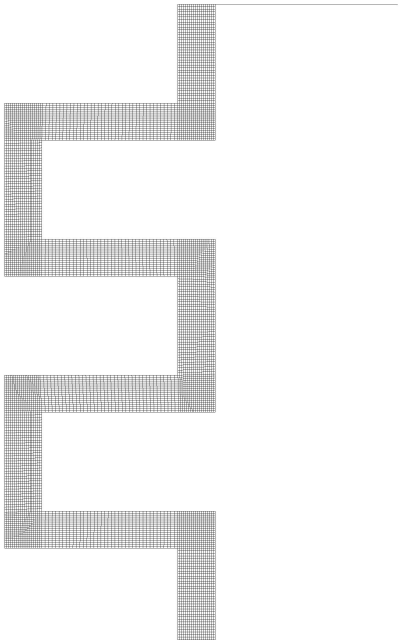

Figure 4: Example of mesh generated for the radial double geometry with 13600 volumes.

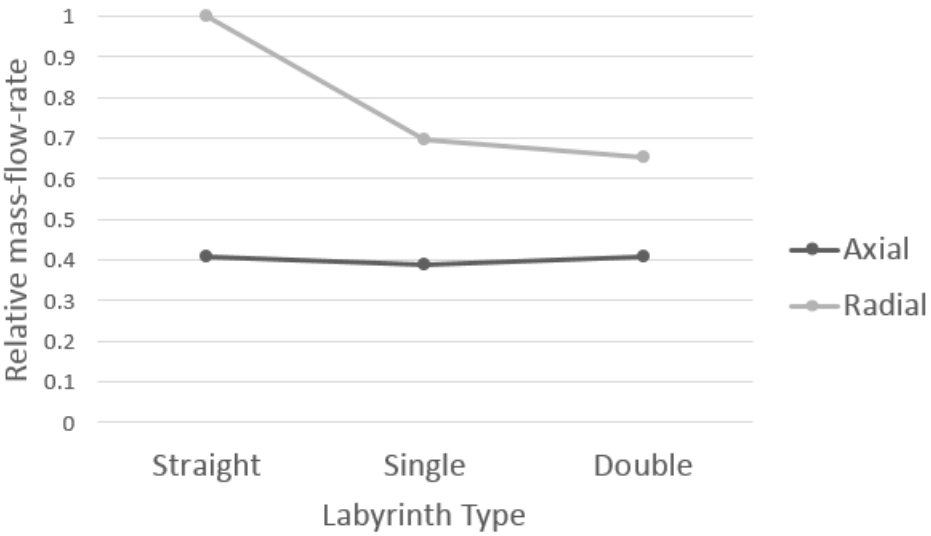

Figure 5: Comparison between analytical and numerical solutions for grease NLGI 2.

As shown in Fig. 7 the angular inclination of the pressure drop for the radial position is similar for both cases, the difference relies on the flow at the axial direction. It is possible to notice that for this direction the pressure drops faster, Figure 8, this phenomena is caused due to the area growth in the radial direction.

The relative mass-flow-rate remains greater on the radial labyrinth due to the centrifugal force, that increases the flow rate in the radial direction.

The following Fig. 9 demonstrate how the dynamic pressure for the axial mounted labyrinth are smaller in comparison with the radial mounted for similar boundary conditions.

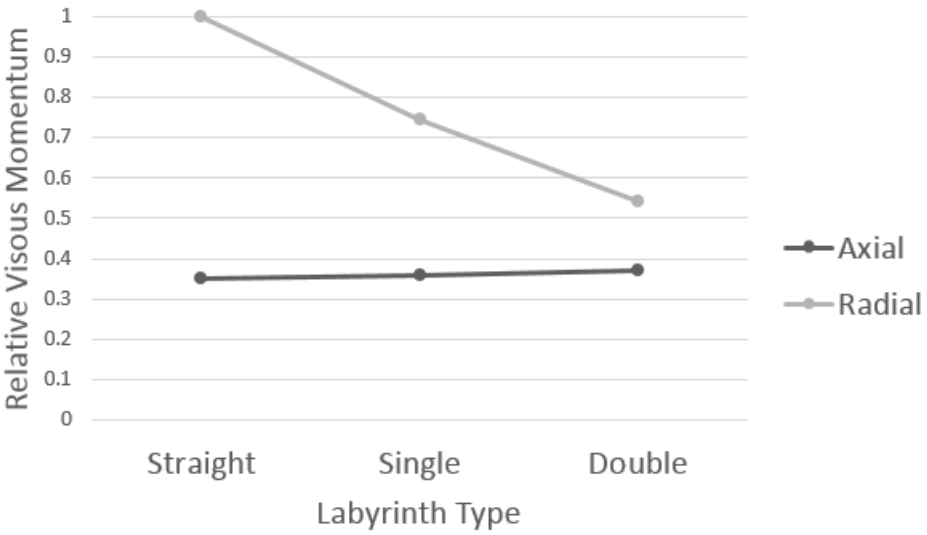

Figure 6: Comparison between analytical and numerical solutions for grease NLGI 2.

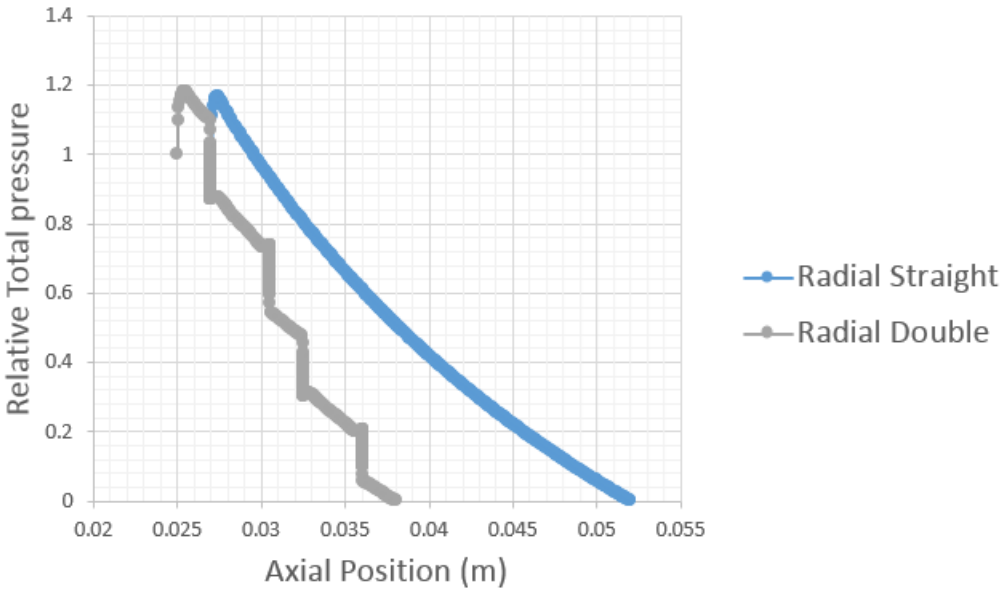

Figure 7: Pressure drop in the axial direction for double radial labyrinth geometry.

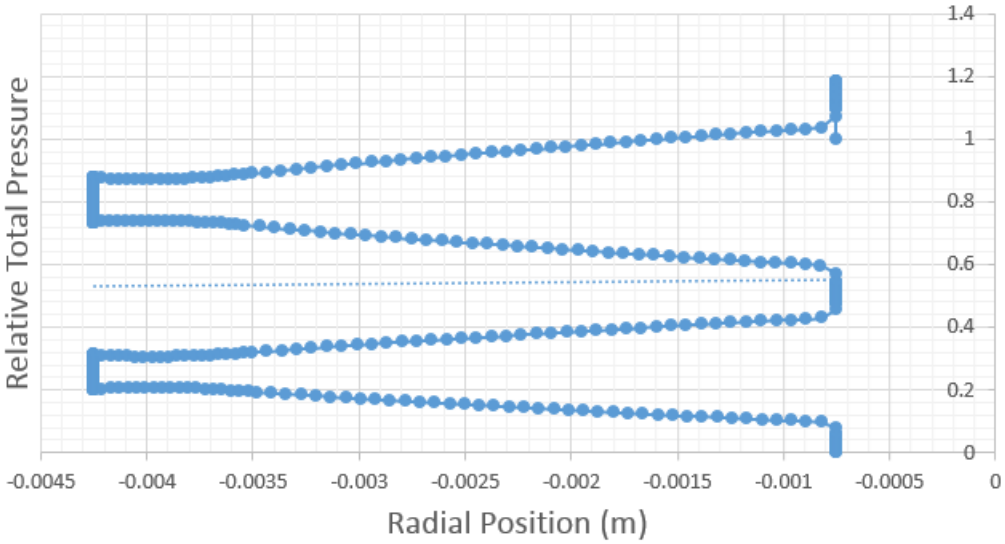

Figure 8: Pressure drop in the radial direction for double axial labyrinth geometry.

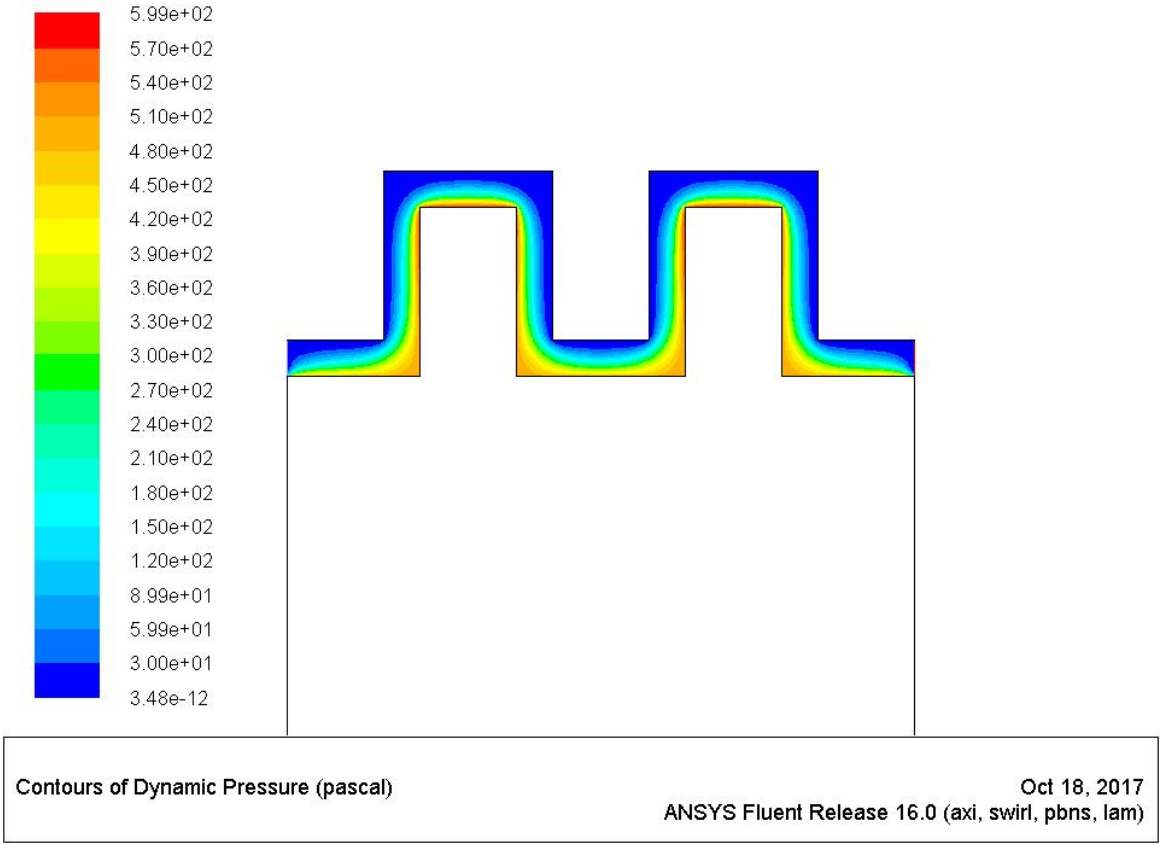

(a) Double axial labyrinth

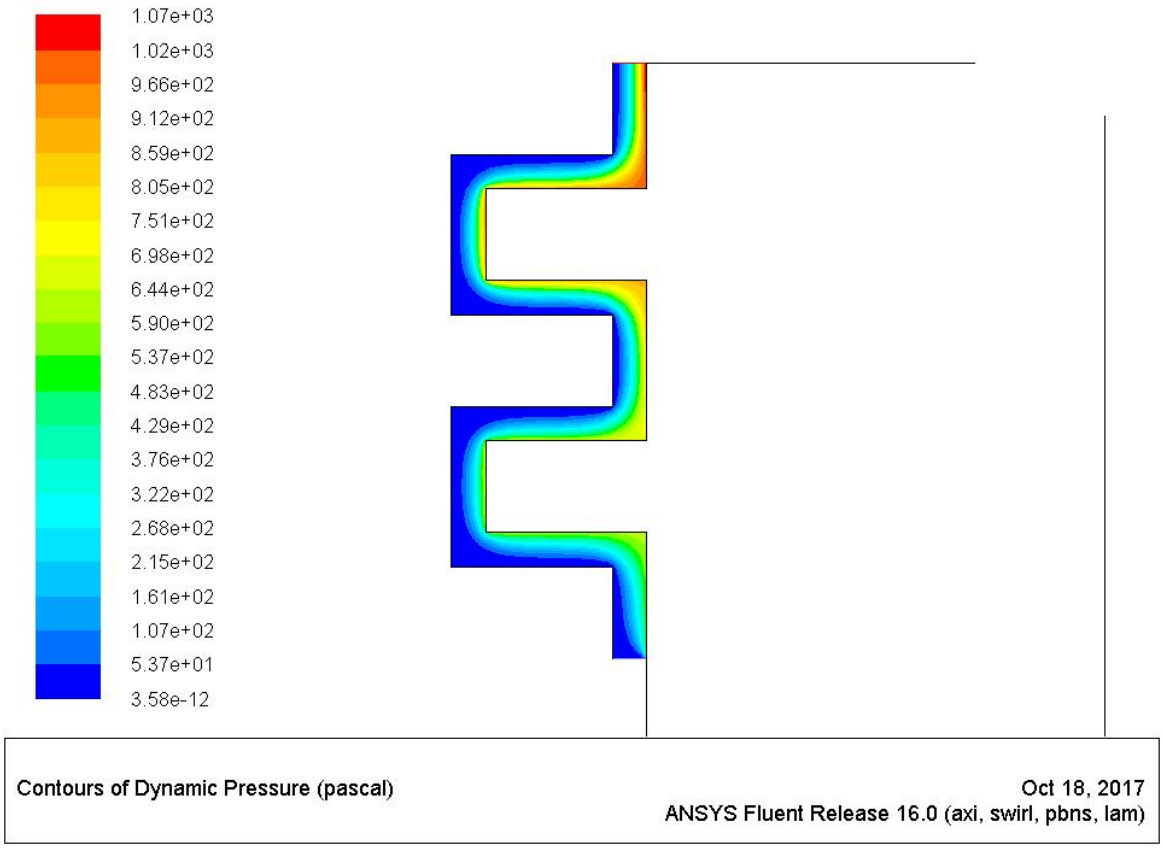

(b) Double axial labyrinth

Figure 9: Dynamic pressure for axial double labyrinth.

4. Conclusions

Numerical simulations of grease have been carried out using FLUENT and successfully validated with the analytical solution of pressure-driven flow between two parallel plates. Several labyrinth geometries have been analyzed using the rheological values of the grease study that considered also shear stresses at low shear rates, resulting in a better approximation for our numerical simulation. The present work have shown a model that could be used to define which labyrinth type should be used for a given application. This optimization can increase the life of the rolling bearing and elevate the project global reliability.

5. REFERENCES

Barnes, H.A. and Walters, K., 1985. "The yield stress myth?" *Rheologica Acta*, Vol. 24, No. 4, pp. 323–326. ISSN 00354511. doi:10.1007/BF01333960.

Cousseau, T., 2013. *Film thickness and friction in grease lubricated contacts. Application to rolling bearing torque loss*. Ph.D. thesis, Universidade do Porto.

Dobrowolski, J.D., Gawliński, M., Paszkowski, M., Westerberg, L.G. and Höglund, E., 2016. "Experimental Study of Lubricating Grease Flow inside the Gap of a Labyrinth Seal Using Microparticle Image Velocimetry". *Tribology Transactions*, Vol. 0, No. 0, pp. 1–10. ISSN 1040-2004. doi:10.1080/10402004.2016.1271928. URL https://www.tandfonline.com/doi/full/10.1080/10402004.2016.1271928.

Fernandes, R.R., 2015. *Relação Entre o Limite de Viscoeslasticidade Linear e o Limite de Escoamento de um Material Elastoviscoplástico*. Ph.D. thesis, Universidade Tecnológica Federal do Paraná.

Gonçalves, D., Marques, R., Graça, B., Campos, A.V., Seabra, J.H.O., Leckner, J. and Westbroek, R., 2015. "Formulation, rheology and thermal aging of polymer greases - Part II: Influence of the co-thickener content". *Tribology International*, Vol. 87, pp. 171–177. ISSN 0301679X. doi:10.1016/j.triboint.2015.01.012. URL http://dx.doi.org/10.1016/j.triboint.2015.01.012.

Kümmel, J. and Werner, H., 2010. "Fettgefüllte Berührungsfreie Wellendichtungen. Berührungsfreie Wellendichtungen mit Fettfüllung zur Schmutzabdichtung". *Abschlussbericht*, , No. Frankfurt.

Lars Westerberg, Erik Höglund, C.S., 2016. "Modelling and experimental validation of lubricating grease flow". *Luleå University of Technology*, Vol. 1, p. 23.

Miskovic, Z., Mitrovic, R. and Stamenic, Z., 2016. "Analysis of grease contamination influence on the internal radial clearance of ball bearings by thermographic inspection". *Thermal Science*, Vol. 20, No. 1, pp. 255–265. ISSN 0354-9836. doi:10.2298/TSCI150319083M. URL http://www.doiserbia.nb.rs/Article.aspx?ID=0354-98361500083M.

Nguyen, Q. D. D., V.B.D., 1992. "MEASURING THE FLOW PROPERTIES OF YIELD STRESS FLUIDS". *Victoria*, pp. 47–88. ISSN 02636050.

Westerberg, L.G., Sarkar, C., Farre, J. and Lundstro, T.S., 2017. "Lubricating Grease Flow in a Double Restriction Seal Geometry : A Computational Fluid Dynamics Approach". doi:10.1007/s11249-017-0864-2.

6. RESPONSIBILITY NOTICE

The authors are the only responsible for the printed material included in this paper.